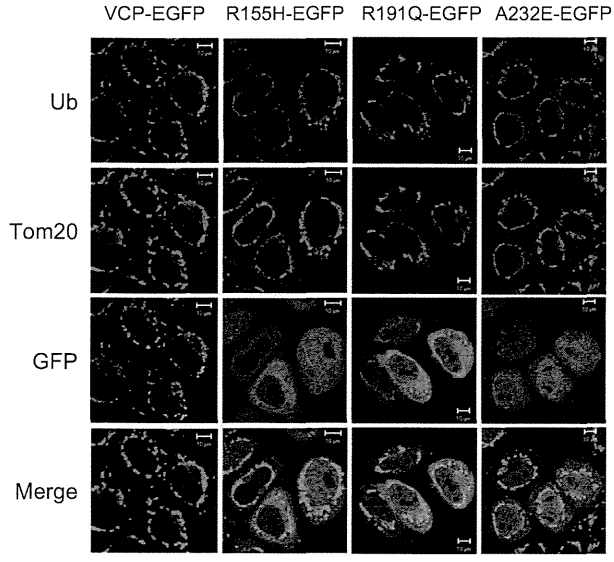

Figure 5 Ubiquitin accumulation on mitochondria in HA-Parkin-expressing HeLa cells after CCCP treatment. Cells that expressed VCP-EGFP or pathogenic VCP-EGFPs were stained with anti-ubiquitin and anti-Tom20 antibodies. GFP fluorescence indicates VCP-EGFP or pathogenic VCP-EGFP expression. Scale bars = 10 μm.

2010), we initially speculated that pathogenic VCPs might prevent mitochondria ubiquitination, which would result in the impaired mitochondria localization by pathogenic VCPs. However, mitochondria ubiquitination efficiently occurred after CCCP treatment of cells that expressed paVCP-EGFP, similar to that in wtVCP-GFP-expressed cells (Fig. 5). This indicated that pathogenic VCPs did not move to mitochondria even though mitochondria were ubiquitinated.

Because pathogenic VCPs can bind to cofactors, such as Npl4, Ufd1 or p47, more efficiently than wild-type VCP (Fernandez-Saiz & Buchberger 2010; Manno *et al.* 2010), we examined whether paVCP-EGFPs expression affected the localization of endogenous Npl4 and p47 after CCCP treatment. We found that Npl4 and p47 exhibited rather diffuse staining patterns due to paVCP-EGFP expression (Fig. 6). These results suggested that pathogenic VCPs prevented these cofactors from moving to mitochondria after CCCP treatment.

Morphological analyses of control flies and flies expressing wild-type VCP or pathogenic VCPs

To investigate the roles of wild-type and pathogenic VCPs in mitochondrial quality control in a different

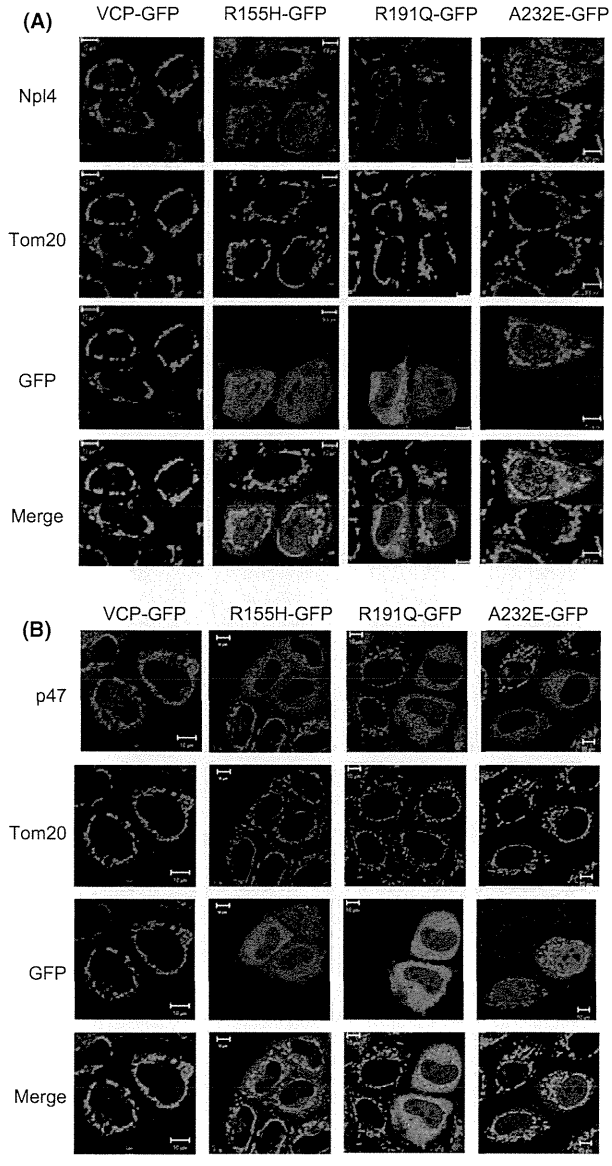

Figure 6 Localization of Npl4 and p47 in cells that express VCP-EGFP or pathogenic VCP-EGFPs. After 2 h of CCCP treatment, cells were stained with anti-Npl4 (A), anti-p47 (B) and anti-Tom20 antibodies (A and B). GFP fluorescence indicates VCP-GFP or pathogenic VCP-GFPs expression. Scale bars = 10 μm.

manner, we used electron microscope to morphologically examine the dorsal longitudinal muscle (DLM), a part of the flight muscle of control and flies expressing human wild-type VCP or pathogenic VCP(R155H). In the flight muscle, many mitochondria are longitudinally aligned between myofibrils, and the cristae in each mitochondrion are tightly packed and in an orderly structure.

In 20-day-old control flies, however, we occasionally observed mitochondria with abnormal morphologies (Fig. 7A). In these mitochondria, a part of cristae lost tightly packed structures and often assumed swirl-like structures. These swirl-like structures looked similar to those that had been reported in the flight muscle of aging blowflies, in the flight muscle of flies after exposure to hyperemia and in the mitochondria of cells with mutations of mitochondria components (Sacktor & Shimada 1972; Walker & Benzer 2004; John *et al.* 2005). In many cases, these aberrant structures were associated with functional mitochondrial defects.

EM photomicrographs were taken for a part of DLM from the dorsal side to the ventral side across a DLM, and the proportion of mitochondria with the aberrant cristae structures among the total mitochondria was calculated (Fig. 7B, Fig. S2, Table S1 in supporting information). This showed that when wild-type VCP was expressed, the proportion of mitochondria with aberrant cristae structures decreased. However, in a VCP(R155H)-expressing fly, this effect was not observed. We confirmed that wild-type VCP and VCP(R155H) were similarly expressed (Fig. 7C). These results suggested that the expression of wild-type VCP, but not that of VCP(R155H), may have a protective role against the aberrant mitochondria formation in *Drosophila* flight muscles.

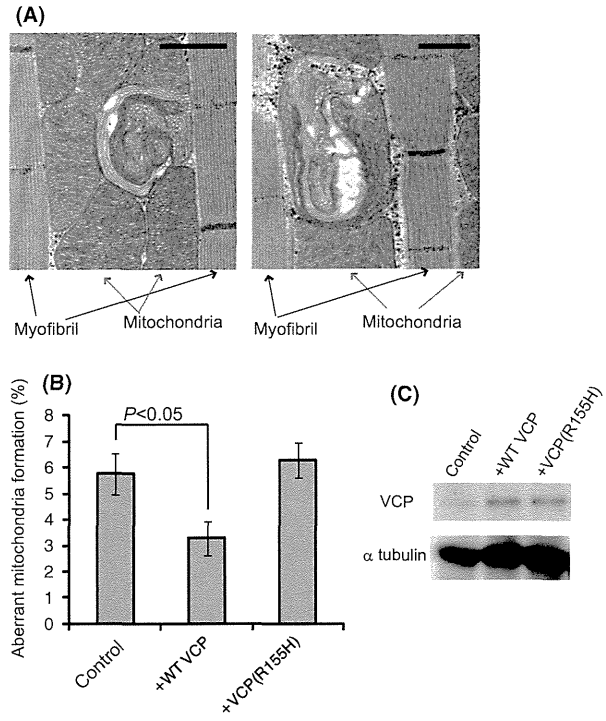

Figure 7 Mitochondrial morphology analyses of control flies and flies expressing wild-type VCP or pathogenic VCP. (A) Electron micrographs of flight muscles with typical mitochondria and aberrant structures observed in 20-day-old control flies. Myofibrils and mitochondria regions are indicated. Scale bars = 1 μm. (B) Quantification of a ratio of the aberrant mitochondria in flight muscle of control flies and flies expressing VCP or VCP(R155H). Ratios of abnormal mitochondria out of all the mitochondria were calculated. Results are means ± SEs of three (control), five (+WT VCP) and four flies [+VCP(R155H)]. (C) Expression levels of VCPs and α-tubulin in control flies and flies that expressed VCP or VCP (R155H) were examined by Western blotting.

Discussion

In this study, we examined the movements of wild-type and pathogenic VCPs, and VCP cofactors to mitochondria. Based on these findings and previous studies, we propose models for wild-type and pathogenic VCP movements (Fig. 8). The first model is based on reports showing that Npl4/Ufd1 can assume two forms in a cell: a VCP-bound and a VCP-free form (Meyer *et al.* 2000), and that Npl4/Ufd1 efficiently binds ubiquitin chains independent of VCP (Ye *et al.* 2003). We speculate that with balanced binding to VCP in the normal state, VCP-free Npl4/Ufd1 surveys for ubiquitinated proteins within a cell. Once mitochondria become ubiquitinated, VCP-free Npl4/Ufd1 may detect and bind to ubiquitinated proteins on mitochondria and subsequently recruit VCP. Because pathogenic VCPs bind to Npl4/Ufd1 more efficiently than wild-type VCP, the equilibrium for binding may shift toward VCP-bound Npl4/Ufd1. In this case, VCP-free Npl4/Ufd1 may be insufficient to detect ubiquitinated proteins, which would result in inadequate recruitment of pathogenic VCPs to mitochondria. We showed that more 'a large fraction of mitochondria' remained in Ufd1 siRNA-treated cells than in VCP siRNA-treated cell (Fig. 3D,E), supporting the idea that Ufd1 might be involved in not only VCP-mediated but also VCP-independent mechanisms (e.g., detecting ubiquitinating proteins in the first place), for the elimination of damaged mitochondria.

Another model assumes that pathogenic VCPs in conjunction with Npl4/Ufd1 bind to ubiquitinated proteins so efficiently that pathogenic VCP/Npl4/Ufd1 can barely bind to any more ubiquitinated proteins, whereas wild-type VCP/Npl4/Ufd1 can still bind to ubiquitinated proteins on mitochondria. However, because VCP is a hexamer and can form a

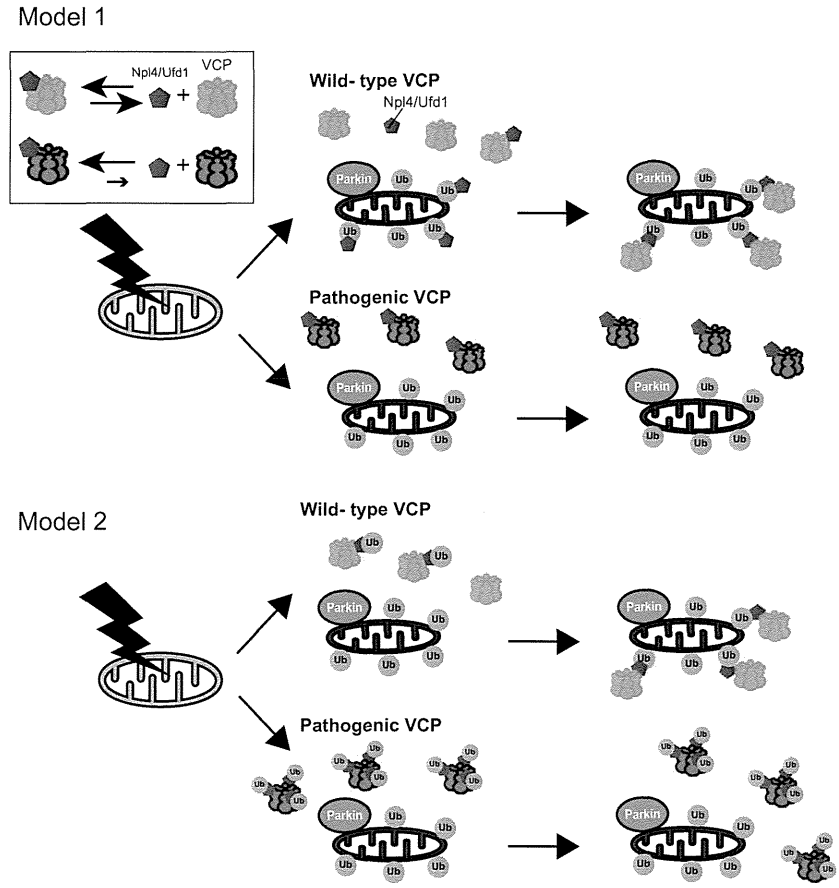

Figure 8 Two models to account for different movements of wild-type and pathogenic VCP. Model 1: In the normal state, wild-type VCP binding to Npl4/Ufd1 occurs in an equilibrium, and Npl4/Ufd1 assumes two forms: VCP-bound and VCP-free forms. When mitochondria are highly ubiquitinated, VCP-free Npl4/Ufd1 detects and binds ubiquitinated proteins on mitochondria. Next, VCP is recruited to Npl4/Ufd1 on mitochondria. Pathogenic VCP binds tightly to Npl4/Ufd1, and binding equilibrium is shifted toward VCP-bound Npl4/Ufd1 form. Thus, few VCP-free Npl4/Ufd1 are available to detect ubiquitin accumulation on mitochondria. Model 2: Wild-type VCP/Npl4/Ufd1 binds to less ubiquitinated proteins than pathogenic VCP/Npl4/Ufd1 in the normal state. Wild-type VCP/Npl4/Ufd1 complexes are recruited to ubiquitinated mitochondria because they can bind to new ubiquitinated proteins on mitochondria. Pathogenic VCP/Npl4/Ufd1 complexes are already occupied with ubiquitinated proteins so that they are unable to efficiently bind new ubiquitinated proteins on mitochondria. Wild-type VCP is indicated in pink and pathogenic VCP in red.

mixed hexamer comprising wild-type and pathogenic VCPs, the scenario for VCP movement might be complicated. As the ratio of wild-type to pathogenic promoters increases, these mixed hexamers might be able to move to mitochondria and behave like a wild-type VCP hexamer. In addition, some other unidentified factor(s), such as Vms1 in yeast, may be involved in recruiting VCP to mitochondria in mammalian systems (Heo *et al.* 2010). Therefore, additional experiments are required to elucidate the molecular mechanisms of VCP movement in detail.

Kim *et al.* (2013) reported that transfected GFP-tagged Npl4 localized to mitochondria in Parkin-expressing cells after CCCP treatment and that Npl4 and Ufd1 were required for damaged mitochondria clearance. Their results were consistent with those of the present study. They also showed that GFP-tagged Ufd1 co-localized with mitochondria after CCCP treatment and that over-expression of pathogenic VCP(A232E) inhibited damaged mitochondria clearance, which showed functional defects in the mitochondrial quality control by pathogenic VCPs.

In their study, exogenously expressed EGFP-tagged p47 did not co-localize with mitochondria after CCCP treatment, whereas we found that endogenous p47 did migrate to mitochondria. We

checked the specificity of our anti-p47 antibody used for the immunofluorescence analysis using p47 siRNA-treated cells (Fig. S3 in supporting information). In p47 siRNA-treated cells, mitochondria-merged staining was not observed. In addition, we did not observe exogenously expressed EGFP-tagged p47 co-localization with Tom20, which was consistent with the results of Kim *et al.* (our unpublished results). Thus, the different results for p47 localization might have been because exogenously expressed EGFP-tagged p47 did not respond to CCCP. Moreover, in contrast to the findings of Kim *et al.* that p47 did not play a role in clearing mitochondria after CCCP treatment, we observed defective mitochondria clearance by p47 siRNA-treated cells, which suggested that p47 played a role in the later stage of mitochondria clearance, possibly during mitophagy. The reason for the different results is unknown. It may be that our cell line was more sensitive to the effect of p47 depletion than their cell lines.

In our analysis of mitochondria in flight muscles, we showed that mitochondria with aberrant structures decreased when wild-type VCP, but not pathogenic VCP, was exogenously expressed. These results suggested that VCP, but not pathogenic VCP, functions in clearing damaged mitochondria or in preventing the formation of aberrant mitochondria. This was compatible with the recent reports that mice with the homozygous and heterologous pathogenic mutations exhibited mitochondria abnormalities (Nalbandian *et al.* 2012; Yin *et al.* 2012). In addition, Bartolome *et al.* (2013) recently published a paper reporting that fibroblasts from patients with IBMPFD had mitochondrial uncoupling, which resulted in reduced cellular ATP levels and established mitochondria dysfunctions in pathogenic VCP-expressing cells.

In conclusion, we showed different behaviors between wild-type and pathogenic VCP, and this behaviors may be related to the pathogenesis of IBMPFD and ALS.

Experimental procedures

Cell culture and transfections

HeLa cells that stably expressed HA-tagged Parkin were generated using recombinant retroviruses as described previously (Okatsu *et al.* 2012). The retroviral receptor mCAT1 was transiently expressed in HeLa cells before viral infection. Cells were maintained in Dulbecco's modified Eagle's medium (DMEM) supplemented with glucose and L-glutamine (Sigma) and containing penicillin/streptomycin, 10% fetal bovine serum (FBS; Gibco) and puromycin (5 μg/ml) at 37 °C with 5% CO_2. Transfection for transient expression used Fugene 6 (Roche), and cells were cultured for 1 day. To depolarize mitochondria, cells were treated with 10 μM CCCP for 2 h.

Plasmids and siRNAs

VCP-EGFP and mutant plasmids were described previously (Manno *et al.* 2010).

For siRNA analysis, siRNAs (VCP ncds sense and VCP ncds antisense, Npl4 679 and Npl4 679 antisense, Ufd1 216 sense and Ufd1 216 antisense, p47 1477 sense and p47 1477 antisense) (Manno *et al.* 2010) were treated using Lipofectamine RNAiMAX reagent (Invitrogen) for 2 days (2 h of CCCP treatment) and for 1.5 days (16 h of CCCP treatment). Control siRNA sequence is as follows: 5′-rCrGrUrUrArA rUrCrG rCrGrUrArUrArArUrArCrGrCrGrUrArU-3′, 5′-rArUrArCrGrCrGrUrArUrUrArUrArC rGrCrGrArUrUrArArCrG-3′.

Transgenic flies

UAS-wtVCP and UAS-VCP(R155H) transgenic flies were generated as described previously (Manno *et al.* 2010). Their genotypes were as follows: Act5c-Gal4/+, Act5c-Gal4/+; UAS-wtVCP/+(wtVCP), Act5c-Gal4/+; UAS-VCP[R155H]/+ [VCP(R155H)].

Electron microscopy

Thoraces were removed from adult flies and fixed in 2% glutaraldehyde plus 2% paraformaldehyde with 0.1 M sodium cacodylate buffer overnight at 4 °C. Samples were embedded, sectioned at 70 nm thickness and stained with 2% uranyl acetate. The preparations were examined under a transmission electron microscope (JEOL JEM-1200EX). Because more abnormal mitochondria tended to be observed at the ventral than at the dorsal side, images were acquired from the dorsal across the ventral side of the DLM as shown in Fig. S2 in supporting information. For each fly, four regions were chosen from the dorsal to the ventral sides as indicated in red squares. In some flies, two areas were taken as for region four to obtain a sufficient area. Six images were acquired for each region.

Statistical analyses of fly mitochondria

For quantification, the number of mitochondria with aberrant structures having diameters of >0.67 μm and total mitochondria were counted from the six images, from which the ratios of aberrant to total mitochondria were calculated (Table S1). To statistically compare the ratios of control and VCP-expressing flies, a t-test of mean equality using the ratios from all the four regions was performed. The analysis showed that VCP-expressing flies had significantly fewer abnormal mitochondria than the control flies ($P = 0.0212$). This result was confirmed using a nonparametric Kruskal–Wallis test that rejected that

the two samples were from the same population ($P = 0.0067$). Finally, to correct for potential differences between the regions, we used linear regression for the ratios of abnormal mitochondria. VCP-expressing flies had significantly 2.5% fewer abnormal mitochondria than the controls after controlling for regions ($P = 0.009$; adj. $R^2 = 0.36$).

Immunocytochemistry

Cell fixation and immunostaining were performed as described previously (Matsuda *et al.* 2010). In brief, cells were fixed with 4% paraformaldehyde for 5 min and permeabilized with 50 μg/ml of digitonin. After blocking with 0.1% gelatin in PBS, cells were incubated with primary antibodies followed by secondary antibodies: anti-mouse or anti-rabbit Alexa Fluor 488, 568 and 647 (Invitrogen). Cells were imaged using a laser-scanning confocal microscope (LSM510; Carl Zeiss, Inc.).

Affinity-purified rabbit polyclonal anti-VCP, anti-p47 and anti-Npl4 antibodies used for immunofluorescent staining were developed previously (Hirabayashi *et al.* 2001; Noguchi *et al.* 2005). In brief, rabbits were immunized with purified recombinant GST fusion proteins. Next, rabbit serum was incubated with GST protein and *E coli* lysates to remove antibodies against GST and *E. coli* proteins. Subsequently, antibodies were affinity-purified against GST fusion proteins for each cofactor or VCP. Antibodies used were as follows: anti-HA (F7, Santa Cruz), anti-GFP (Invitrogen), polyclonal anti-ubiquitin (DAKO) and anti-Tom20 (FL-145 or FL-10, Santa Cruz) antibodies.

To quantify the localizations of various VCP-EGFPs, cells were imaged by microscope, and approximately 100–200 transfected cells were examined in each experiment. For cells that expressed wild-type VCP-EGFP, a small portion of cells showed aberrant mitochondria localization and morphology after CCCP treatment. These cells were not counted.

Immunoblotting

Parkin-expressing HeLa cells were washed with PBS twice, and a cell monolayer was lysed for 5 min in RIPA buffer with 0.1% SDS supplemented with complete protease inhibitor cocktail (Roche) plus 1 mM NEM and then cleared for 10 min at 15,000 × *g*.

To compare the amounts of exogenous VCPs in flies, whole-body lysates of each genotype were analyzed by Western blotting. Lysates were prepared using lysis buffer [50 mM Tris pH 7.4, 19 mM NaF, 5 mM EDTA, supplemented with protease inhibitor cocktail (NACALAI TESQUE), and 1 mM PMSF] at 4 °C. Mouse monoclonal anti-VCP antibody, which specifically recognized mammalian VCP, used for Fig. 7, was produced by standard procedure using mouse immunized with full-length VCP-fused KLH.

Antibodies used were as follows: antimitofusin 1(Abnova), antimitofusin 2 (Abcam), anti-GFP (Invitrogen), anti-actin (AC-40, Sigma) and antitubulin (DM1a, Santa Cruz).

Acknowledgements

We thank Tokai Electronic Cooperation for EM analysis, H. Akabayashi for statistical analyses and the members of the Tanaka laboratory for helpful discussions. This work was supported in part by Grants-in-Aids for Scientific Research (C), Specially Promoted Research, Scientific Research on Innovative Areas (to Y.K.), a JSPS KAKENHI Grant Number 23-6061 (to K.O., for JSPS Fellows) and research grants from the Ministry of Education, Culture, Sports, and Technology of Japan, and by Solution Oriented Research for Science and Technology from the Japan Science Technology Agency (JST).

References

Bartolome, F., Wu, H.C., Burchell, V.S., *et al.* (2013) Pathogenic VCP mutations induce mitochondrial uncoupling and reduced ATP levels. *Neuron* **78**, 57–64.

Braun, R.J., Zischka, H., Madeo, F., Eisenberg, T., Wissing, S., Buttner, S., Engelhardt, S.M., Buringer, D. & Ueffing, M. (2006) Crucial mitochondrial impairment upon CDC48 mutation in apoptotic yeast. *J. Biol. Chem.* **281**, 25757–25767.

Chan, N., Le, C., Shieh, P., Mozaffar, T., Khare, M., Bronstein, J. & Kimonis, V. (2012) Valosin-containing protein mutation and Parkinson's disease. *Parkinsonism Relat Disord.* **18**, 107–109.

Erzurumlu, Y., Kose, F.A., Gozen, O., Gozuacik, D., Toth, E.A. & Ballar, P. (2013) A unique IBMPFD-related P97/VCP mutation with differential binding pattern and subcellular localization. *Int. J. Biochem. Cell Biol.* **45**, 773–782.

Fernandez-Saiz, V. & Buchberger, A. (2010) Imbalances in p97 co-factor interactions in human proteinopathy. *EMBO Rep.* **11**, 479–485.

Freibaum, B.D., Chitta, R.K., High, A.A. & Taylor, J.P. (2010) Global analysis of TDP-43 interacting proteins reveals strong association with RNA splicing and translation machinery. *J. Proteome Res.* **9**, 1104–1120.

Halawani, D., LeBlanc, A.C., Rouiller, I., Michnick, S.W., Servant, M.J. & Latterich, M. (2009) Hereditary inclusion body myopathy-linked p97/VCP mutations in the NH2 domain and the D1 ring modulate p97/VCP ATPase activity and D2 ring conformation. *Mol. Cell. Biol.* **29**, 4484–4494.

Heo, J.M., Livnat-Levanon, N., Taylor, E.B., Jones, K.T., Dephoure, N., Ring, J., Xie, J., Brodsky, J.L., Madeo, F., Gygi, S.P., Ashrafi, K., Glickman, M.H. & Rutter, J. (2010) A stress-responsive system for mitochondrial protein degradation. *Mol. Cell* **40**, 465–480.

Higashiyama, H., Hirose, F., Yamaguchi, M., Inoue, Y.H., Fujikake, N., Matsukage, A. & Kakizuka, A. (2002) Identification of ter94, Drosophila VCP, as a modulator of polyglutamine-induced neurodegeneration. *Cell Death Differ.* **9**, 264–273.

Hirabayashi, M., Inoue, K., Tanaka, K., Nakadate, K., Ohsawa, Y., Kamei, Y., Popiel, A.H., Sinohara, A., Iwamatsu,

A., Kimura, Y., Uchiyama, Y., Hori, S. & Kakizuka, A. (2001) VCP/p97 in abnormal protein aggregates, cytoplasmic vacuoles, and cell death, phenotypes relevant to neurodegeneration. *Cell Death Differ.* **8**, 977–984.

Janiesch, P.C., Kim, J., Mouysset, J., Barikbin, R., Lochmuller, H., Cassata, G., Krause, S. & Hoppe, T. (2007) The ubiquitin-selective chaperone CDC-48/p97 links myosin assembly to human myopathy. *Nat. Cell Biol.* **9**, 379–390.

Jentsch, S. & Rumpf, S. (2007) Cdc48 (p97): a "molecular gearbox" in the ubiquitin pathway? *Trends Biochem. Sci.* **32**, 6–11.

John, G.B., Shang, Y., Li, L., Renken, C., Mannella, C.A., Selker, J.M., Rangell, L., Bennett, M.J. & Zha, J. (2005) The mitochondrial inner membrane protein mitofilin controls cristae morphology. *Mol. Biol. Cell* **16**, 1543–1554.

Johnson, J.O., Mandrioli, J., Benatar, M., *et al.* (2010) Exome sequencing reveals VCP mutations as a cause of familial ALS. *Neuron* **68**, 857–864.

Ju, J.S., Miller, S.E., Hanson, P.I. & Weihl, C.C. (2008) Impaired protein aggregate handling and clearance underlie the pathogenesis of p97/VCP-associated disease. *J. Biol. Chem.* **283**, 30289–30299.

Kim, N.C., Tresse, E., Kolaitis, R.M., *et al.* (2013) VCP is essential for mitochondrial quality control by PINK1/Parkin and this function is impaired by VCP mutations. *Neuron* **78**, 65–80.

Kimonis, V.E., Kovach, M.J., Waggoner, B., Leal, S., Salam, A., Rimer, L., Davis, K., Khardori, R. & Gelber, D. (2000) Clinical and molecular studies in a unique family with autosomal dominant limb-girdle muscular dystrophy and Paget disease of bone. *Genet Med.* **2**, 232–241.

Kimura, Y. & Kakizuka, A. (2003) Polyglutamine diseases and molecular chaperones. *IUBMB Life* **55**, 337–345.

Kondo, H., Rabouille, C., Newman, R., Levine, T.P., Pappin, D., Freemont, P. & Warren, G. (1997) p47 is a cofactor for p97-mediated membrane fusion. *Nature* **388**, 75–78.

Krick, R., Bremer, S., Welter, E., Schlotterhose, P., Muehe, Y., Eskelinen, E.L. & Thumm, M. (2010) Cdc48/p97 and Shp1/p47 regulate autophagosome biogenesis in concert with ubiquitin-like Atg8. *J. Cell Biol.* **190**, 965–973.

Manno, A., Noguchi, M., Fukushi, J., Motohashi, Y. & Kakizuka, A. (2010) Enhanced ATPase activities as a primary defect of mutant valosin-containing proteins that cause inclusion body myopathy associated with Paget disease of bone and frontotemporal dementia. *Genes Cells* **15**, 911–922.

Matsuda, N., Sato, S., Shiba, K., Okatsu, K., Saisho, K., Gautier, C.A., Sou, Y.S., Saiki, S., Kawajiri, S., Sato, F., Kimura, M., Komatsu, M., Hattori, N. & Tanaka, K. (2010) PINK1 stabilized by mitochondrial depolarization recruits Parkin to damaged mitochondria and activates latent Parkin for mitophagy. *J. Cell Biol.* **189**, 211–221.

Meyer, H., Bug, M. & Bremer, S. (2012) Emerging functions of the VCP/p97 AAA-ATPase in the ubiquitin system. *Nat. Cell Biol.* **14**, 117–123.

Meyer, H.H., Shorter, J.G., Seemann, J., Pappin, D. & Warren, G. (2000) A complex of mammalian ufd1 and npl4 links the AAA-ATPase, p97, to ubiquitin and nuclear transport pathways. *EMBO J.* **19**, 2181–2192.

Nalbandian, A., Llewellyn, K.J., Kitazawa, M., Yin, H.Z., Badadani, M., Khanlou, N., Edwards, R., Nguyen, C., Mukherjee, J., Mozaffar, T., Watts, G., Weiss, J. & Kimonis, V.E. (2012) The homozygote VCP(R(1)(5)(5)H/R(1)(5)(5)H) mouse model exhibits accelerated human VCP-associated disease pathology. *PLoS ONE* **7**, e46308.

Narendra, D., Tanaka, A., Suen, D.F. & Youle, R.J. (2008) Parkin is recruited selectively to impaired mitochondria and promotes their autophagy. *J. Cell Biol.* **183**, 795–803.

Narendra, D.P., Jin, S.M., Tanaka, A., Suen, D.F., Gautier, C.A., Shen, J., Cookson, M.R. & Youle, R.J. (2010) PINK1 is selectively stabilized on impaired mitochondria to activate Parkin. *PLoS Biol.* **8**, e1000298.

Noguchi, M., Takata, T., Kimura, Y., Manno, A., Murakami, K., Koike, M., Ohizumi, H., Hori, S. & Kakizuka, A. (2005) ATPase activity of p97/valosin-containing protein is regulated by oxidative modification of the evolutionally conserved cysteine 522 residue in Walker A motif. *J. Biol. Chem.* **280**, 41332–41341.

Nowis, D., McConnell, E. & Wojcik, C. (2006) Destabilization of the VCP-Ufd1-Npl4 complex is associated with decreased levels of ERAD substrates. *Exp. Cell Res.* **312**, 2921–2932.

Okatsu, K., Oka, T., Iguchi, M., *et al.* (2012) PINK1 autophosphorylation upon membrane potential dissipation is essential for Parkin recruitment to damaged mitochondria. *Nat. Commun.* **3**, 1016.

Okatsu, K., Saisho, K., Shimanuki, M., Nakada, K., Shitara, H., Sou, Y.S., Kimura, M., Sato, S., Hattori, N., Komatsu, M., Tanaka, K. & Matsuda, N. (2010) p62/SQSTM1 cooperates with Parkin for perinuclear clustering of depolarized mitochondria. *Genes Cells* **15**, 887–900.

Ritson, G.P., Custer, S.K., Freibaum, B.D., Guinto, J.B., Geffel, D., Moore, J., Tang, W., Winton, M.J., Neumann, M., Trojanowski, J.Q., Lee, V.M., Forman, M.S. & Taylor, J.P. (2010) TDP-43 mediates degeneration in a novel Drosophila model of disease caused by mutations in VCP/p97. *J. Neurosci.* **30**, 7729–7739.

Ritz, D., Vuk, M., Kirchner, P., Bug, M., Schutz, S., Hayer, A., Bremer, S., Lusk, C., Baloh, R.H., Lee, H., Glatter, T., Gstaiger, M., Aebersold, R., Weihl, C.C. & Meyer, H. (2011) Endolysosomal sorting of ubiquitylated caveolin-1 is regulated by VCP and UBXD1 and impaired by VCP disease mutations. *Nat. Cell Biol.* **13**, 1116–1123.

Sacktor, B. & Shimada, Y. (1972) Degenerative changes in the mitochondria of flight muscle from aging blowflies. *J. Cell Biol.* **52**, 465–477.

Schuberth, C. & Buchberger, A. (2008) UBX domain proteins: major regulators of the AAA ATPase Cdc48/p97. *Cell. Mol. Life Sci.* **65**, 2360–2371.

Shibata, Y., Oyama, M., Kozuka-Hata, H., Han, X., Tanaka, Y., Gohda, J. & Inoue, J. (2012) p47 negatively regulates IKK activation by inducing the lysosomal degradation of polyubiquitinated NEMO. *Nat. Commun.* **3**, 1061.

Stolz, A., Hilt, W., Buchberger, A. & Wolf, D.H. (2011) Cdc48: a power machine in protein degradation, *Trends Biochem. Sci.* **36**, 515–523.

Takata, T., Kimura, Y., Ohnuma, Y., Kawawaki, J., Kakiyama, Y., Tanaka, K. & Kakizuka, A. (2012) Rescue of growth defects of yeast cdc48 mutants by pathogenic IBMPFD-VCPs. *J. Struct. Biol.* **179**, 93–103.

Tanaka, A., Cleland, M.M., Xu, S., Narendra, D.P., Suen, D.F., Karbowski, M. & Youle, R.J. (2010) Proteasome and p97 mediate mitophagy and degradation of mitofusins induced by Parkin. *J. Cell Biol.* **191**, 1367–1380.

Tang, W.K., Li, D., Li, C.C., Esser, L., Dai, R., Guo, L. & Xia, D. (2010) A novel ATP-dependent conformation in p97 N-D1 fragment revealed by crystal structures of disease-related mutants. *EMBO J.* **29**, 2217–2229.

Vives-Bauza, C., Zhou, C., Huang, Y., *et al.* (2010) PINK1-dependent recruitment of Parkin to mitochondria in mitophagy. *Proc. Natl Acad. Sci. USA* **107**, 378–383.

Walker, D.W. & Benzer, S. (2004) Mitochondrial "swirls" induced by oxygen stress and in the Drosophila mutant hyperswirl. *Proc. Natl Acad. Sci. USA* **101**, 10290–10295.

Watts, G.D., Wymer, J., Kovach, M.J., Mehta, S.G., Mumm, S., Darvish, D., Pestronk, A., Whyte, M.P. & Kimonis, V.E. (2004) Inclusion body myopathy associated with Paget disease of bone and frontotemporal dementia is caused by mutant valosin-containing protein. *Nat. Genet.* **36**, 377–381.

Weihl, C.C., Dalal, S., Pestronk, A. & Hanson, P.I. (2006) Inclusion body myopathy-associated mutations in p97/VCP impair endoplasmic reticulum-associated degradation. *Hum. Mol. Genet.* **15**, 189–199.

Xu, S., Peng, G., Wang, Y., Fang, S. & Karbowski, M. (2011) The AAA-ATPase p97 is essential for outer mitochondrial membrane protein turnover. *Mol. Biol. Cell* **22**, 291–300.

Ye, Y., Meyer, H.H. & Rapoport, T.A. (2003) Function of the p97-Ufd1-Npl4 complex in retrotranslocation from the ER to the cytosol: dual recognition of nonubiquitinated polypeptide segments and polyubiquitin chains. *J. Cell Biol.* **162**, 71–84.

Yin, H.Z., Nalbandian, A., Hsu, C.I., Li, S., Llewellyn, K.J., Mozaffar, T., Kimonis, V.E. & Weiss, J.H. (2012) Slow development of ALS-like spinal cord pathology in mutant valosin-containing protein gene knock-in mice. *Cell Death Dis.* **3**, e374.

Ziviani, E., Tao, R.N. & Whitworth, A.J. (2010) Drosophila parkin requires PINK1 for mitochondrial translocation and ubiquitinates mitofusin. *Proc. Natl Acad. Sci. USA* **107**, 5018–5023.

Received: 18 August 2013
Accepted: 12 September 2013

Supporting Information

Additional Supporting Information may be found in the online version of this article at the publisher's web site:

Figure S1 Large images of control siRNA-and Ufd1-siRNA treated cells stained with anti-VCP and anti-Tom20 antibodies.

Figure S2 *Drosophila* flight muscle sections used to evaluate mitochondria morphology.

Figure S3 Anti-p47 antibody specificity.

Table S1 Summary of mitochondria analyses of *Drosophila* flight muscle